A novel adaptive PD-type iterative learning control of the PMSM servo system with the friction uncertainty in low speeds

Saleem Riaz[1], **Rong Qi**[1], **Onder Tutsoy**[2], **Jamshed Iqbal**[3]*

1 School of Automation, Northwestern Polytechnical University, Shaanxi, Xi'an, PR China, **2** Department of Electrical-Electronics Engineering, Adana Alparslan Turkes Science and Technology University, Adana, Türkiye, **3** School of Computer Science, Faculty of Science and Engineering, University of Hull, Hull, United Kingdom

* j.iqbal@hull.ac.uk

Abstract

High precision demands in a large number of emerging robotic applications strengthened the role of the modern control laws in the position control of the Permanent Magnet Synchronous Motor (PMSM) servo system. This paper proposes a learning-based adaptive control approach to improve the PMSM position tracking in the presence of the friction uncertainty. In contrast to most of the reported works considering the servos operating at high speeds, this paper focuses on low speeds in which the friction stemmed deteriorations become more obvious. In this paper firstly, a servo model involving the Stribeck friction dynamics is formulated, and the unknown friction parameters are identified by a genetic algorithm from the offline data. Then, a feedforward controller is designed to inject the friction information into the loop and eliminate it before causing performance degradations. Since the friction is a kind of disturbance and leads to uncertainties having time-varying characters, an Adaptive Proportional Derivative (APD) type Iterative Learning Controller (ILC) named as the APD-ILC is designed to mitigate the friction effects. Finally, the proposed control approach is simulated in MATLAB/Simulink environment and it is compared with the conventional Proportional Integral Derivative (PID) controller, Proportional ILC (P-ILC), and Proportional Derivative ILC (PD-ILC) algorithms. The results confirm that the proposed APD-ILC significantly lessens the effects of the friction and thus noticeably improves the control performance in the low speeds of the PMSM.

1. Introduction

Recent emerging advancements in the automation technology have redefined the role of the robotics and mechatronics systems in modern-day industrial world. To perform various tasks like the welding, machine tending, grinding, packaging, assembling and material transporting, a variety of robots such as the industrial robot manipulators [1], wheeled mobile robots [2] and track-driven mobile robots [3] have been widely considered. Owing to stringent requirements of the precision and accuracy in a highly nonlinear and dynamic environments, there is an increasing demand to develop novel actuation and control technologies for these industrial robots [4, 5].

The PMSM has been broadly used in industrial robots, high-precision CNC machines, and other applications employing servo control due to its small size, simple structure, low moment of inertia, and high-power density. It is reported that the servo control systems performing repetitive tasks can theoretically achieve satisfactory tracking results using the ILC [6]. However, various disturbances, modeling errors [7], and time-varying system parameters [8] adversely affect the convergence of the ILC. Therefore, the control community is actively working on the ILC-based control of the PMSM servo systems working under the dynamic uncertainties [9]. Recently, researchers have combined the adaptive control and ILC to form Adaptive Iterative Learning Control (AILC) [10, 11], which exploits the ILC to solve the repetitive tracking problems [12, 13] and adaptive control to handle the system uncertainty problem. Thus, AILC improves the tracking accuracy of the PMSM servo system and also accelerates the controller speed of convergence in the presence of the uncertainties [14, 15].

Compared with the 'traditional rotating motor and ball screw' drive mode, a Permanent Magnet Linear Synchronous Motor (PMLSM) adopts a direct-drive mode, without any conversion links in the middle and offers larger thrust, low loss, and fast response. Owing to these advantages, the PMLSM has been widely preferred in a large number of industrial applications [16–18]. However, the parametric changes, friction, measurement disturbances, and cogging force affect the motor motion which cause formidable control challenges. This necessitates a robust controller design with an ability to accurately track the reference trajectory by eliminating the detrimental effects of the uncertainties [19, 20].

Due to the uncertainties in the PMSM servo system, its high precision tracking control with the conventional PID controller is challenging [21–23]. In addition, owing to the nature of underlying mathematical structure, it is not easy to fully compensate the nonlinearities of the motor with the linear control approaches having constant gains [24, 25]. Work reported in [26] expressed that a disturbance predictor-based control can improve the tracking accuracy of the controller since it gains the disturbance rejection capability. Another work [27] employed an iterative learning approach to reduce the controller position gain in order to enhance the position tracking of a linear motor working in specific state intervals. However, increase in the number of iterations reduced the controller convergence speed [28]. Similarly, an open-loop P-type ILC for the compensation of the measurement noise has been presented in [29]. The non-repetitive disturbance considerably fluctuated the motor position since the controller was unable to handle the instant random changes in the disturbance [30, 31].

Other types of control approaches without the friction disturbances are the intelligent control [32], adaptive fuzzy control [33] and Active Disturbance Rejection Control (ADRC) [34]. The Disturbance Observer (DOB) compensation methods are reviewed in [35]. The neural network control algorithm in [32] and the fuzzy control algorithm in [33, 36, 37] have approximated the friction characteristics by a genetic algorithm. A controller was then designed to compensate the friction. However, due to the hardware constraints, the intelligent control algorithm requires a large amount of online computations. The primary DOB disturbance compensation method in [38] and its counterpart ADRC in [34, 39] both suppressed the friction, but their dynamic performances and stability analyses were not carried out [40, 41].

In scientific literature, the PMSM vector control system has been established on the *dq*-axis transformed model with $i_d = 0$ in which the transformed *d*-axis current (i_d) of the PMSM is kept at zero to ease the control problem. Generally, the influence of the uncertain factors such as the friction torque, cogging torque, modelling errors, and the time-varying parameters on the control system have been analyzed. The well-known state equations of the system have been established. Recently, a parametric AILC law has been formulated to lessens the deteriorations in the PMSM servo system's tracking accuracy and error divergence caused by the

model uncertainty. The primary method is to add adaptive iterative feature to the PD-based feedback control law. Through the parameter learning, the unknown parameters of the control law are identified. Then, based on the previous learning law, an enhanced version of the adaptive iterative learning law is presented. This corresponds to adding a time-domain estimate of the unknown parameters to the former learning law while taking full advantage of the information in both the continuous and discrete times.

Given the nonlinear approximation ability of the neural networks, a number of researchers have used them to identify the frictional torque and compensate it with the controller [42–45]. The neural network can be either used as the central controller or is combined with other control algorithms to gain adaptive control properties [46]. The robustness of the controller against the friction and other disturbances has been demonstrated in [47, 48] which present suitable entropy-based ILC compensation and in [49, 50] where various ILC approaches are introduced. Fuzzy control with adaptive internal model control can also be used as a disturbance suppression approach. For example, in [51, 52] an improved internal model control is utilized for the speed control and two disturbance observers estimate the moment of inertia and the PMSM load. In [51], the motor disturbances have observed by the combination of an uncertainty predictor and a state predictor. Its feedforward compensation has been applied to the control system by using the uncertainty predictor estimates which leads to a superior control performance. A further research reported in [53] presented a hybrid control scheme based on sliding mode control and disturbance rejection of a second order PMSM system whose efficiency has been demonstrated through experimental validation.

In recent years, a number of researchers have adopted robust adaptive control, especially the adaptive backstepping law, to achieve high accuracy in servo control [54–57]. Majority of the reported works considered the motor's high speed and thus an improvement in performance at relatively low speeds is still an open research area. This paper focuses on the control of the PMSM running at low speeds where the friction Stribeck compensation problem occurs. To handle the identified friction uncertainty, the APD-ILC position control algorithm, which is an iterative and adaptive control approach, is developed. Simulations are performed to qualitatively analyze the results and verify the position tracking and the friction compensation abilities of the APD-ILC algorithm.

The control algorithm incorporates the friction model in the form of the feedforward control to generate a friction-free APD-ILC algorithm. The typical ILC relies on powerful mathematical calculations instead of precise models. On the other hand, the degree of function compensation is primarily determined by the filter's bandwidth, which is restricted by variables such as the mechanical resonance in the system. Consequently, there is a limited capacity to adjust for friction nonlinearity at zero speed. Basically, the proposed technique updates the learning gain of the controller according to the magnitude of the error to improve the tracking accuracy of the system. At the same time, the exponential learning gain is introduced into the differential coefficient of the controller to speed up the convergence. Finally, the efficiency of the proposed control technique is demonstrated in simulation.

This article is divided into five sections. Section 2 derives the model of a PMSM, Section 3 provides the convergence analysis, theory of adaptive ILC, nonlinear gain function, and the sufficient conditions for the error convergence Section 4 presents simulation results to validate the proposed control approach and finally, Section 5 concludes the paper.

2. Permanent Magnet Synchronous Motor System (PMSM) model

This research considers a surface-mounted PMSM model transformed in the dq-axis. The typical PMSM mathematical model is given in Eq (1), which uses the notations presented in

Table 1. Nomenclature.

Notation	Description
T_e	Electromagnetic torque
K_m	Equivalent gain of the PMSM driver
$u(t)$	Control input
θ	Motor angular position
ω	Motor angular speed
J_m	Total inertia
B_m	Damping coefficient
T_L	Loading torque
$\eta(t)$	Random measurement noise
$x(t)$	System states
A,B,C,E,D	System vectors and matrices
F	System friction torque
h	Sampling time
I	Identity matrix with appropriate dimension
$y_d = \theta_d(t)$	Desired position trajectory
k	Current iteration index
e_k	Tracking error
y_k	System actual output
K_P	Proportional gain
K_D	Derivative gain
u_k	Output of the APD-ILC controller
K_1	ILC proportional learning gain
K_2	ILC derivative learning gain
Δe_k	Sample differenced tracking error
τ_P, τ_D	Positive constant gains
k_1	Upper bound of nonlinear function $f(.)$
k_0	Lower bound of nonlinear function $f(.)$
α, b_d, b_η	Positive scaling numbers

Table 1.

$$\begin{cases} \dfrac{di_d}{dt} = -\dfrac{R_s}{L_d}i_d + \dfrac{L_q}{L_d}n_p\omega i_q + \dfrac{1}{L_d}u_d \\[2mm] \dfrac{di_q}{dt} = -\dfrac{R_s}{L_q}i_q - \dfrac{L_d}{L_q}n_p\omega i_d - \dfrac{\psi_f}{L_q}n_p\omega + \dfrac{1}{L_q}u_q \\[2mm] \dfrac{d\omega}{dt} = -\dfrac{B_m}{J}\omega + \dfrac{n_p}{J}\left[\psi_f i_q + (L_d - L_q)i_d i_q\right] \end{cases} \quad (1)$$

where u_d, u_q are the stator voltages and i_d, i_q are the armature currents and the L_d, L_q are the stator inductances on the dq-axis of the motor, n_p is the number of the pole pairs of the PMSM, R_s is the stator resistance, ω is the mechanical angular velocity of the motor rotor, ψ_f is the rotor flux corresponding to the permanent magnet, J is the rotational inertia, B_m is the viscous damping. In the actual system, to decouple the speed and current, the vector control mode of $i_d^* \equiv 0$ is often used. The equation of the electromagnetic torque can be written as:

$$T_e = J\frac{d\omega}{dt} + B_m\omega + T_L = K_t i_q \quad (2)$$

where T_L is the load torque, and K_t is the torque constant.

Let F be the system friction torque, θ be the rotational angle of the motor rotor, J be the sum of the motor and load moment of inertia, then Eq (2) can be re-formulated as:

$$\begin{cases} J\dfrac{d\omega}{dt} = T_e - B_m\omega - T_L - F \\ \dfrac{d\omega}{dt} = \dfrac{1}{J}\left[K_t i_q - B_m\omega - T_L - F\right] \\ \dfrac{d\theta}{dt} = \omega \end{cases} \tag{3}$$

A friction model in [58] is used here to fully describe the friction encountered by the PMSM servo system. The model is represented by the expression;

$$F = (F_c + (F_s - F_c)e^{-(\dot{\theta}/\dot{\theta}_s)})\operatorname{sgn}(\dot{\theta}) + B_m\dot{\theta} \tag{4}$$

where F_c is the Coulomb friction torque, $\dot{\theta}$ is the rotational angular velocity, F_c is the static friction torque, $\dot{\theta}_s$ is the Stribeck characteristic velocity.

2.1 Detailed modelling of the Stribeck friction

Stribeck curve in Fig 1 is a well-known tool for modelling of the friction. It essentially indicates the relationship between the friction force and angular velocity for different values of the
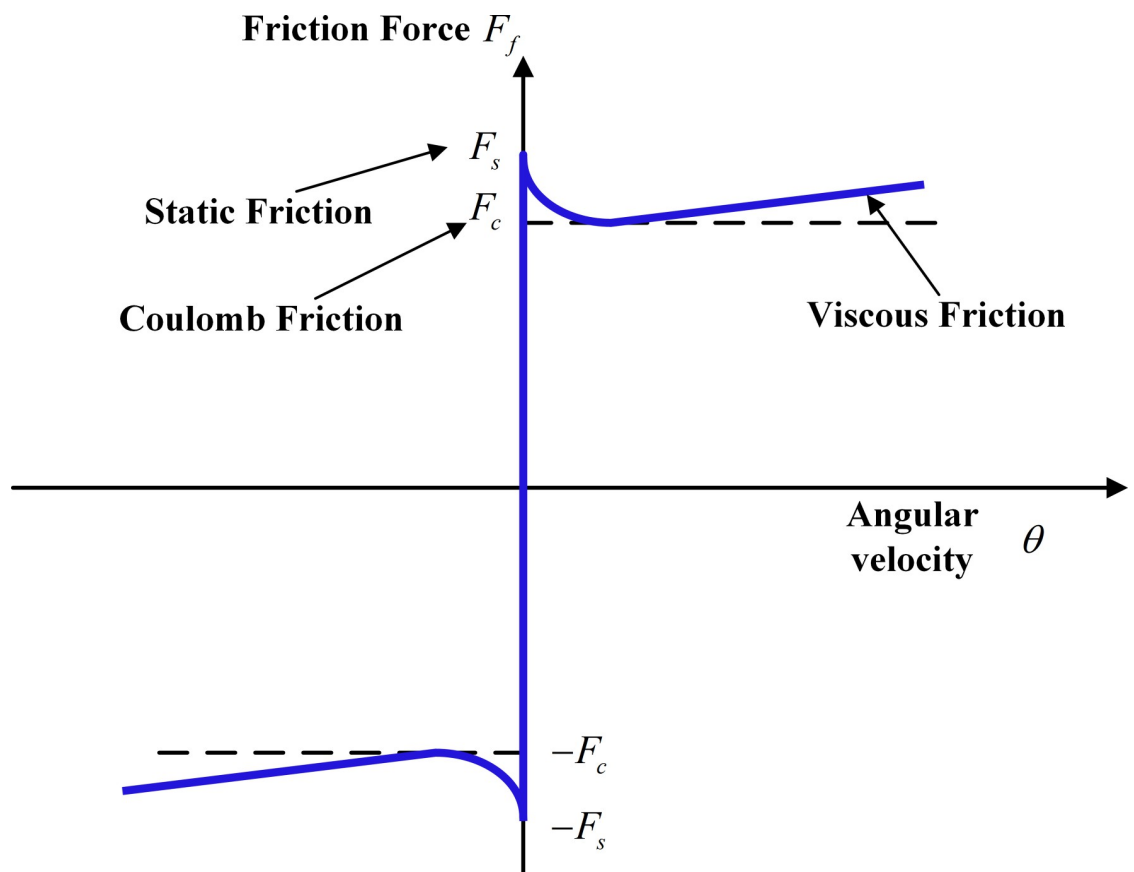
Fig 1. The Stribeck friction curve.

friction. The Stribeck friction model can be expressed as in Eqs (5) and (6). When the static friction is $|\dot{\theta}(t)| < \alpha$, with α threshold, the dynamic friction $F_f(t)$ can be given by (5).

$$F_f(t) = \begin{cases} F_m & F(t) > F_m \\ F(t) & -F_m < F < F_m \\ -F_m & F(t) < -F_m \end{cases} \tag{5}$$

On the other hand, when the static friction is $|\dot{\theta}(t)| > \alpha$, $F_f(t)$ can be given as;

$$F_f(t) = (F_c + (F_m - F_c)e^{-\alpha_1 \dot{\theta}(t)})\text{sgn}(\dot{\theta}(t)) + B_m\dot{\theta} \tag{6}$$

where F_m denotes the driving force, F_c represents the maximum static friction force, α_1 is a small scaling factor.

2.2 Identification of the friction parameters

The genetic algorithm is a probabilistic search optimization approach that imitates the organisms' genetic and evolutionary processes in their natural environment. It can solve complex and poorly known nonlinear optimization problems without requiring the model of the system. The optimization search can be carried out throughout the range of a pre-determined unknown parameter space and the best parameter solutions are selected among them [59]. The genetic algorithm can also avoid local minima with rich and diverse exploration signals, so it gains a wide range of adaptability and strong robustness. Fig 2 shows the overall APD-ILC architecture.

In Fig 2, the desired angular position θ_d^* is compared with the measured angular position θ^* to generate the angular position tracking error. This error is processed by the APD-ILC and the corresponding feedforward control signal is subtracted from the position tracking error weighted with the C_1. This yields a further tracking error which is transformed by the C_2
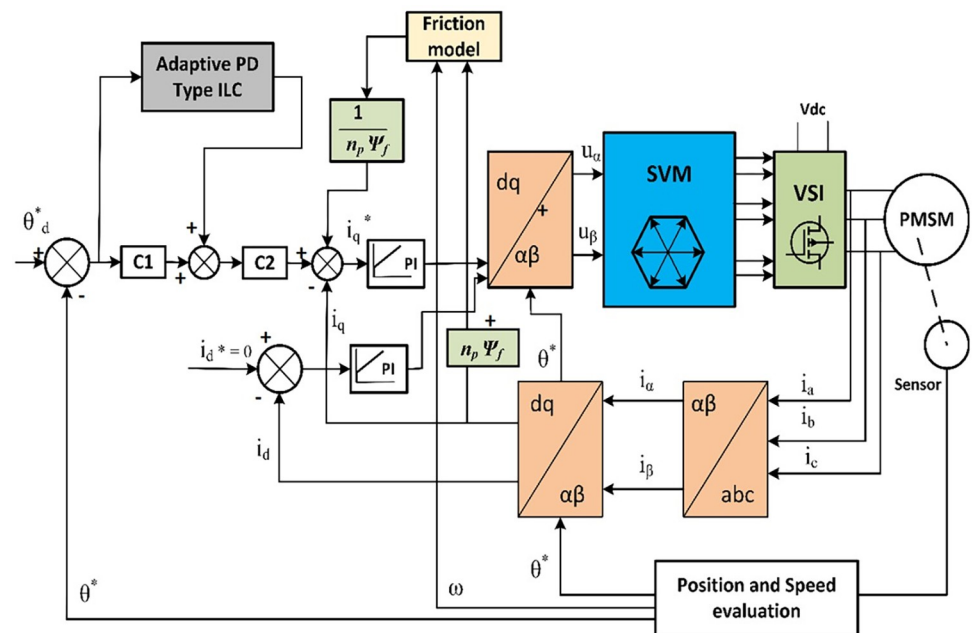
Fig 2. Overall control architecture.

weighting value and compared with the i_q current on the q-axis together with the friction model output to produce the i_q^* desired current. This comparison error is evaluated by the traditional PI controller which feeds the model transformed from dq-axis to $\alpha\beta$-axis. Similarly, in case of the desired current $i_d^* = 0$, a further PI controller assesses the i_d current on the d-axis and provides the control signal for the dq-axis to $\alpha\beta$-axis transformer. The outputs of this transformer are modulated by the Space Vector Modulation (SVM) component and the Voltage Source Inverters (VSI) provides the required 3-phase voltage for the PMSM. When the system is in steady-state, the angular velocity becomes $\dot{\omega} = 0$ and without the load $T_L = 0$, Eq (1) becomes $F = T_e = B_m\omega$.

In terms of the PMSM speed control, consider a set of constant speed $n_p\psi_f$ as the command signal. According to Eq (6), construct the identifier $\hat{F}(x, \dot{\theta}_i)$ and set the parameter to be identified as

$$x = [F_c, F_s, \dot{\theta}, B_m]^T \tag{7}$$

Defining the identification error $e(\dot{\theta}_i, x)$ as;

$$e(\dot{\theta}_i, x) = \sqrt{[F(\dot{\theta}_i) - \hat{F}(x, \dot{\theta}_i)]^2} \tag{8}$$

where

$$F(\dot{\theta}_i) = (F_c + (F_s - F_c)e^{-(\dot{\theta}_i/\dot{\theta}_i)})\mathrm{sgn}(\dot{\theta}_i) + B_m\dot{\theta}_i \tag{9}$$

A quadratic objective function is formulated as:

$$l = \frac{1}{2}\sum_{i=1}^{n} e(\dot{\theta}_i, x)^2 \tag{10}$$

Typically, the traditional optimization methods begin randomly and then iteratively decide on the best result from the solution space. Due to the limited amount of information offered by a single set of training data, the search performance can be poor, and also the search may get locked in the local optimum solution thus entering in stall mode due to insufficient exploration. Properly excited search may help to steadily acquire the global optimal solution by preventing the optimization for superfluous spots and avoiding slipping into the local optimum solution.

Genetic algorithms include selection, crossover and mutation processes and offers a larger likelihood of the global convergence to the optimum solution and a greater capacity to solve the uncertain optimization problems. However, factors such as the crossover probability and mutation probability have an effect on the algorithm's search results and efficiency thus highlighting critical role of the genetic algorithm parameters for a particular application is important.

2.3. Bit string mutation

The mutation of bit strings ensues through bit flips at random positions. For instance:

1	0	1	0	0	1	0
				↓		
1	0	1	0	1	1	0

Definition 1: The *order* of the pattern is the number of 0's and 1's in the pattern and is denoted as $O(H)$ (e.g. $O(11^{*}00^{**}) = 4$.

Definition 2: The *moment* of the pattern, i.e. the length of the pattern, is the distance from the left to right between the first non-* bit and the last non-* bit of the pattern. The moment of the pattern is denoted by $\delta(H)$. e.g.

$$\delta(01**1) = 3; \quad \delta(**0*1) = 2; \quad \delta(***1**) = 1$$

A random number of initial groups encoded with a certain length (which is proportional to the unknown parameter spaces) is created. Each individual is evaluated using the fitness function, and those with a better fitness rating are chosen to engage in the genetic operation, while those with a poor fitness score are removed from the solutions. A group of genetically modified individuals (through replication, crossover, or mutation) generates a new generation population until the stop requirement is fulfilled. The most fully developed person among the descendants is considered to be the outcome of the genetic algorithm. With the mutation, the sequence before the mutation $x = x_1 x_2 \ldots x_i$ might become to $x = x_2 x_1 \ldots x_{i-2}$ for i number of the initial population. The range of each population has a constrained value for each sample k between $[u_{\min}^k, u_{\max}^k]$. The boundaries are implemented on the x_k parameter population as:

$$x_k = \begin{cases} u_{\min}^k & \text{if } random(0,1) = 0 \\ u_{\max}^k & \text{if } random(0,1) = 1 \end{cases}$$

where $random(0,1)$ is generates 0 or 1 values randomly.

The problem of friction parameter identification is to find the parameter vector x in Eq (7) that minimizes the objective function in Eq (10). The decimal floating-point coding format is used for encoding the parameter vector to identify the individual solutions. The selection operation involves a random sampling method that saves the optimal individuals. The overall identified values are compared in Table 2 below. The crossover operation adopts the uniform crossover operator, and the mutation assumes the basic bit. The maximum evolutionary number is 200 with a population size i of 50. The crossover probability is 0.9 and the mutation probability is 0.05. Parameter range F_s is [0,1], F_c is [0,1], B_m is [0,0.05]. Finally, the Stribeck characteristic velocity is $\dot{\theta}_s = [0, 0.05]$.

3. Adaptive ILC-based feedforward controller

According to the Fig 1, the feedforward compensation is achieved in terms of manipulating the motor currents. Eq (2) can be re-written with the friction torque as:

$$J\frac{d\omega}{dt} = -B_m \omega + K_t \left(i_q - i_F\right) - T_L \tag{11}$$

The friction torque F is given by

$$i_F = \frac{F}{K_t} \tag{12}$$

Table 2. Friction identifier parameters.

	F_c	F_s	$\dot{\theta}_s$	B_m
Initial parameters	0.28	0.34	0.01	0.02
Identification results	0.2796	0.3885	0.0108	0.0206

The friction model identified in the section 2.2 is used to perform friction compensation of the PMSM servo system. The proposed feedforward controller is shown in Fig 2. The total control output of the system is sum of the outputs of the PI feedback controllers and the friction feedforward controller given by

$$i_q^* = i_C + i_{\hat{F}} \tag{13}$$

where $i\hat{F} = \frac{\hat{F}}{K_t}$ is the estimated friction torque and i_C is produced by the adaptive ILC. The general control structure is shown in Fig 3.

The PMSM given in Eq (1) with the added Stribeck friction is linearized around the operating points and put in the state space form as:

$$\underbrace{\begin{bmatrix} \dot{\theta} \\ \dot{\omega} \end{bmatrix}}_{\dot{x}(t)} = \underbrace{\begin{bmatrix} 0 & 1 \\ 0 & \dfrac{B_m}{J} \end{bmatrix}}_{A} \underbrace{\begin{bmatrix} \theta \\ \omega \end{bmatrix}}_{x(t)} + \underbrace{\begin{bmatrix} 0 \\ \dfrac{K_t}{J} \end{bmatrix}}_{B} \underbrace{i_q}_{u(t)} + \underbrace{\begin{bmatrix} 0 \\ -\dfrac{T_L + F}{J} \end{bmatrix}}_{d(T_L,T_f)}$$

$$y(t) = \underbrace{\begin{bmatrix} 1 & 0 \end{bmatrix}}_{C} \underbrace{\begin{bmatrix} \theta \\ \omega \end{bmatrix}}_{x(t)} + \eta(t) \tag{14}$$

where A,B,C are the linear system matrices and vectors, $d(T_L,T_F)$ is the disturbances stemmed from the load and the Stribeck friction, $x(t)$ system state vector, $u(t)$ is the controlled i_q current, $\eta(t)$ is the measurement noise type uncertainty. Eq (15) presents the briefed version of the state space representation in Eq (14).

$$\begin{cases} \dot{x}(t) = Ax(t) + Bu(t) + d(T_L, T_f) \\ y(t) = Cx(t) + \eta_t \end{cases} \tag{15}$$

The next sub-section introduces the P-ILC design.

3.1. P-ILC design

A simple control law based on P-ILC is expressed as:

$$\bar{u}_{k+1}(t) = \bar{u}_k(t) + K_P \hat{e}_k(t) \tag{16}$$

where $\bar{u}_{k+1}(t)$ represents the updated control signal and $\hat{e}_k(t)$ is the tracking error.

The well-known condition for the error convergence of the P-ILC algorithm can be described by:

$$\|I - K_p CB\| < 1 \tag{17}$$

The next sub-section provides the APD-ILC algorithm.

3.2. APD-ILC algorithm

Fig 3 presents the configuration of the APD-ILC algorithm applied to the PMSM with the friction uncertainty. In Fig 3, y_d denotes the desired position, y_k represents the output position of the system at $(k+1)^{th}$ iteration, z_{k+1} is the measurement signal at the $(k+1)^{th}$ iteration, e_{k+1} is the position error of $(k+1)^{th}$ iteration, η_{k+1} denotes the disturbance signal.
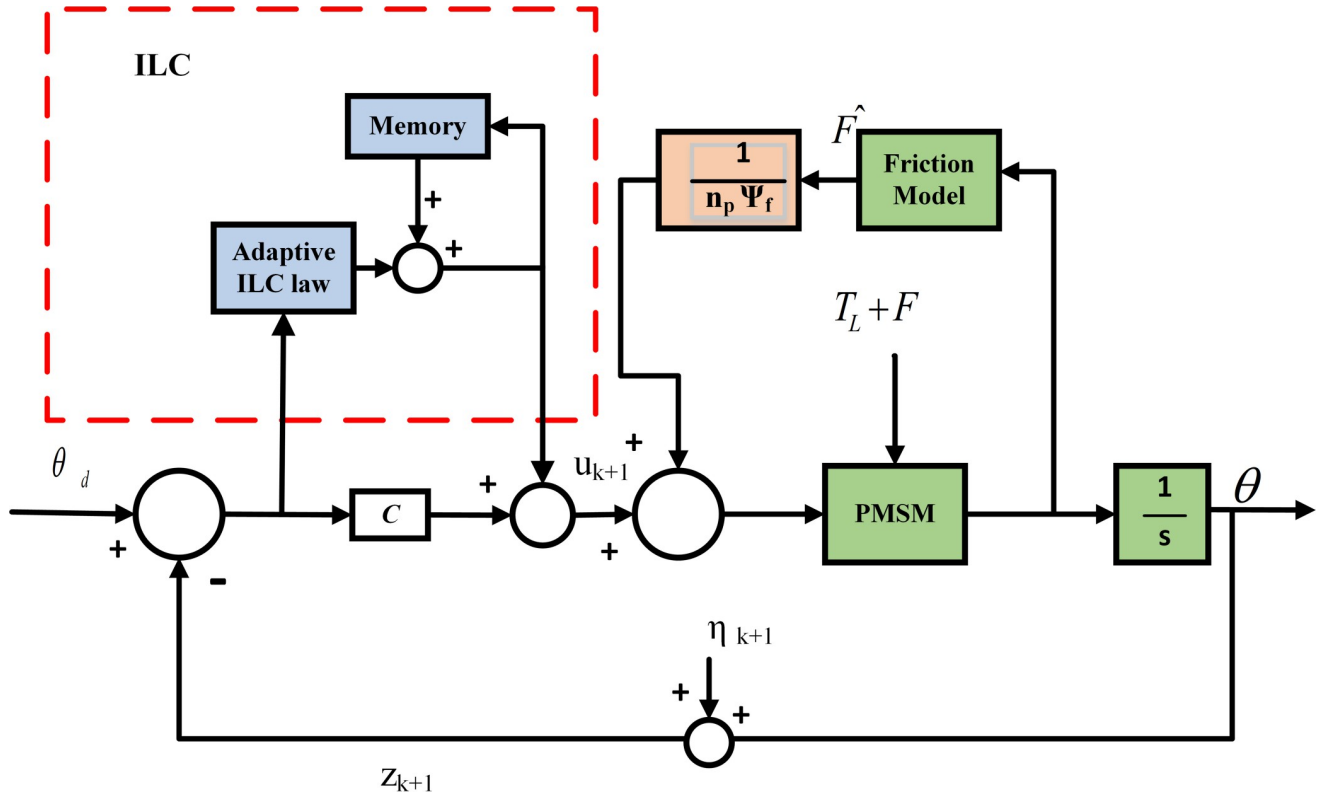
Fig 3. General block diagram illustrating the adaptive ILC-based feedforward controller.

Before analyzing the system, two definitions need to be made. The reference tracking error is defined as:

$$e_k(t) = y_d(t) - z_k(t) \tag{18}$$

The measurement error $\epsilon_k(t)$ is defined as:

$$\epsilon_k(t) = y_d(t) - y_k(t) \tag{19}$$

One can conclude from Fig 1 that $y_k(t) = z_k(t) - \eta_k(t)$ and combining Eqs (18) and (19) yields

$$e_k(t) = \epsilon_k(t) - \eta_k(t) \tag{20}$$

$$\dot{e}_k(t) = \dot{\epsilon}_k(t) - \dot{\eta}_k(t) \tag{21}$$

The traditional PD-ILC law is formulated as:

$$u_{k+1}^0(t) = u_k^0(t) + K_1 e_{k+1}(t) + K_2 \dot{e}_{k+1}(\iota) \tag{22}$$

where K_1 and K_2 are the constant learning gains of the controller. The APD-ILC law with adaptive learning gains is designed as:

$$u_{k+1}(t) = u_k(t) + f(e_{k+1}(t))[K_3 e_{k+1}(t) + K_4 e^{\beta t} e_{k+1}(t)] \tag{23}$$

where $e^{\beta t}$ is an exponential variable gain with $0 < \beta \leq 1$, $f(.)$ is a nonlinear function related to the

error boundary α and changes with the size of the error as:

$$f(e_k) = \begin{cases} 1 - \dfrac{\alpha}{|e_k|} & (|e_k| > \alpha) \\ 0 & (|e_k| \leq \alpha) \end{cases} \tag{24}$$

The resulting curve of the nonlinear error function in Eq (24) is shown in Fig 4.

Remark 1: For the PD-ILC with adaptive learning gains in Eq (22), it is clear that, for $\forall k \in \{0,1,2,\cdots\}$,

$$\begin{cases} K_{1,k} \in [\tau_P k_0, \tau_P k_1] \\ K_{2,k} \in [0, \tau_D k_1] \end{cases} \tag{25}$$

where τ_p and τ_d are the proportional and derivative time constants, k_0 and k_1 are the lower and upper limit scaling factors of the controller gains.

Remark 2: The selection principle of parameter α is as follows: A larger α leads to $f(.)$ with a larger opening concavity, so that a small amplitude of error e_k can lead to a small value of $f(.)$. Therefore, one should determine the value of α according to the amplitude of the random measurement noise, i.e. an error with a small amplitude needs a large α to suppress [60].

The effect of different parameters on the shape of the nonlinear function $f(.)$ and the relationship between $f(.)$ and the error e_k can be seen in Fig 4. As α increases from 0.1 to 0. 5, the $f(e_k)$ function reaches its maximum determined by the upper limit k_1. It shows that the learning gain can be adaptively adjusted for the small errors as well as the large errors. The three curves
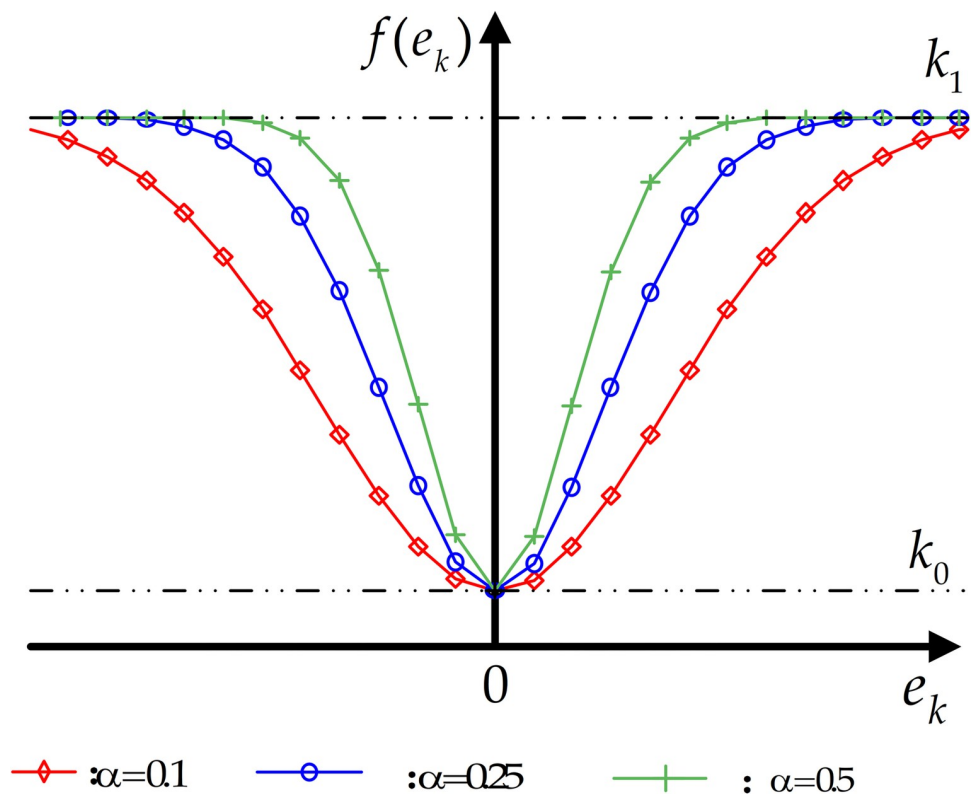
Fig 4. Adaptive gain function.
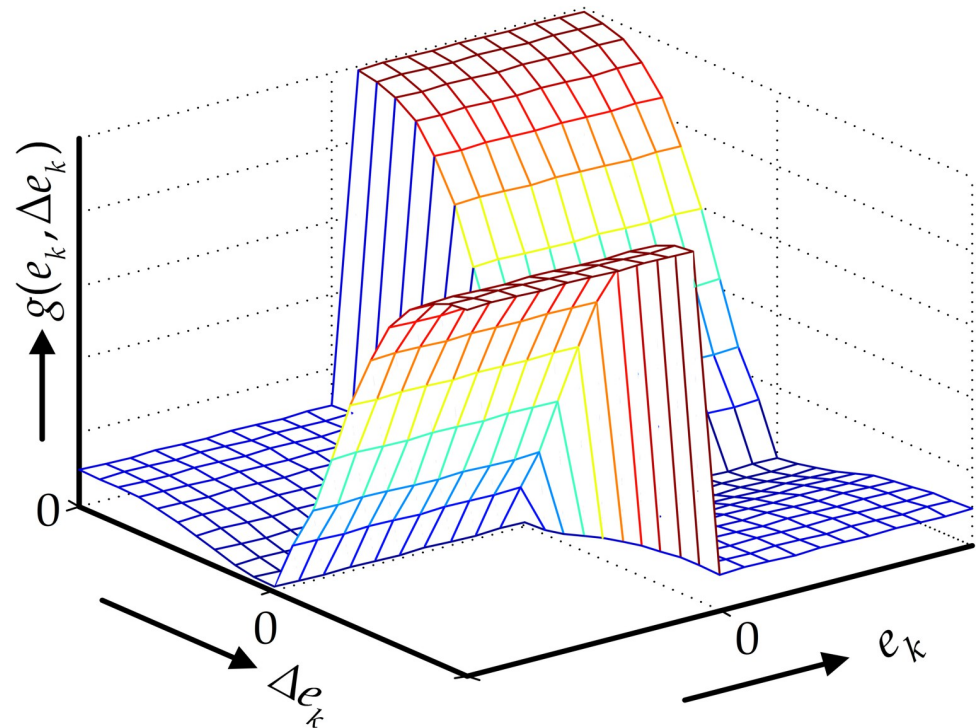
Fig 5. Adaptive nonlinear gain function $g(.)$ versus the sample differenced error Δe_k.

in Fig 4 an show that the error is intuitively adjusted and compensated with the exponential gain function.

The typical nonlinear function $g(e_k, \Delta e_k)$ versus its sample differenced error Δe_k are shown in Fig 5.

In Fig 5, the sample difference error Δe_k has consistent error signs during the learning process of the APD-ILC parameters. This shows that the learning process is smooth due to continuous nature of the control problem and occurs in a stable state region without chattering around the controller operating points.

Changing the damping of the controller or differential learning gain (K_1) improves the adjustment speed and bandwidth of the system. It is stated that when the system error and its differential gains are different, the gains tend to reduce the tracking error. However, when the error and its rate of change are of the same sign, the value of the differential gain is increased which can improve the speed of error convergence and also leads to more stable system. Therefore, to remove the disturbance signal while retaining the useful signal, α should be selected to be smaller than the measurement disturbance amplitude and smaller than the error value of the amplitude.

4. Simulation results and discussions

Three control algorithms are simulated in MATLAB/Simulink environment to validate the effect of friction compensation proposed in this paper. These algorithms are the conventional PID control without feedforward compensation, P-ILC and APD-ILC algorithms. The parameters of the PMSM considered in this paper are given in Table 3.

The controller and filter parameters are given in Table 4.

Table 3. Parameters of the PMSM.

Parameter	Symbol	Value	Unit
Viscous friction coefficient	B_m	0.003	$N.m.s$
Electromagnetic torque	T_e	10	$N.m$
Angular velocity	$\omega(t)$	3000	rad/s
Motor rotor inertia	J	1.7810^{-4}	$Kg/_{m^2}$
Armature winding inductance	$L_d = L_q$	4	mH
Armature winding resistance	R_s	1.74	Ω
Number of pole pairs	n_p	4	-
Permanent magnet flux linkage	ψ_f	0.402	Wb

Table 4. Controller and filter parameters.

Element	Description
	Limit: -15A
Current loop	PI Controller
	Proportional gain = 50
	Integral gain = 2500
	PI Controller
Speed loop	Proportional gain = 1
	Integral gain = 10
Position loop	P Controller
	Proportional gain = 200
ILC filter	Time constant t = 0.001 sec
Reference position signal	$y_d(t) = \sin(t)$ rad
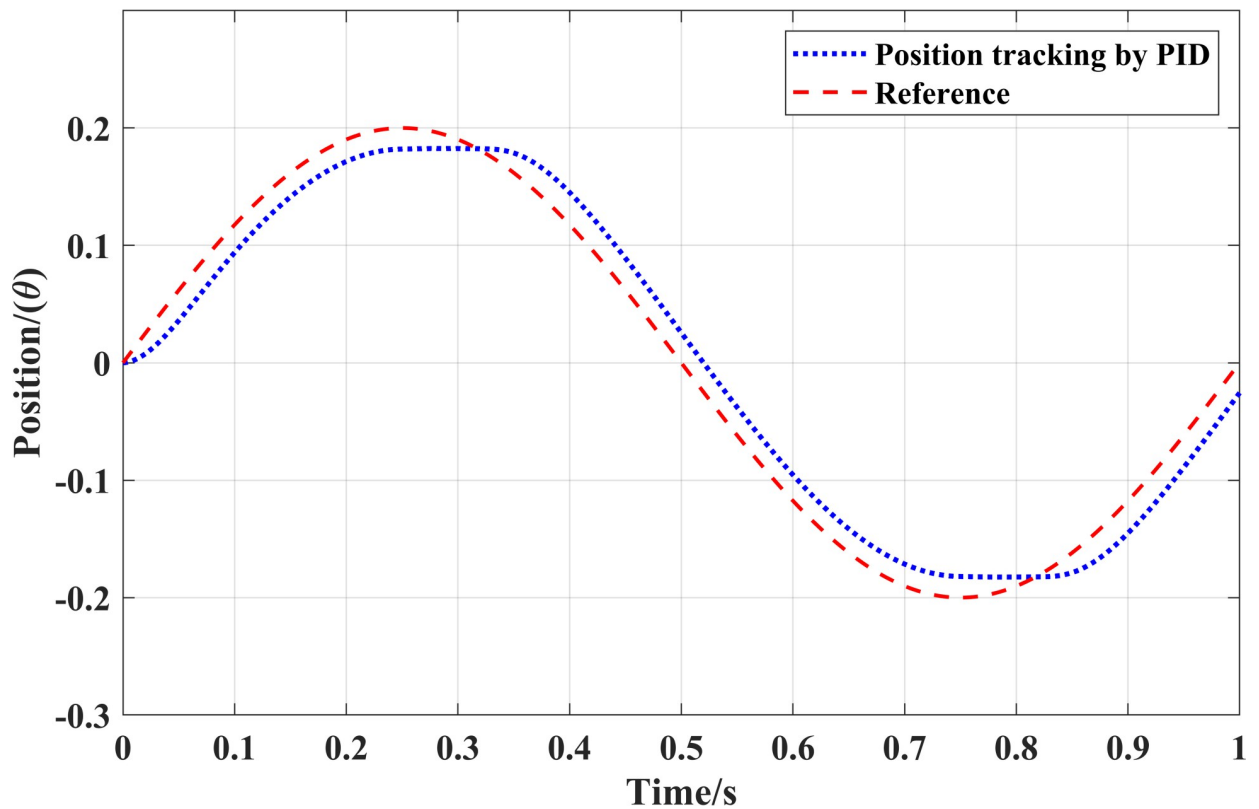
Fig 6. Reference position tracking with the conventional PID controller.
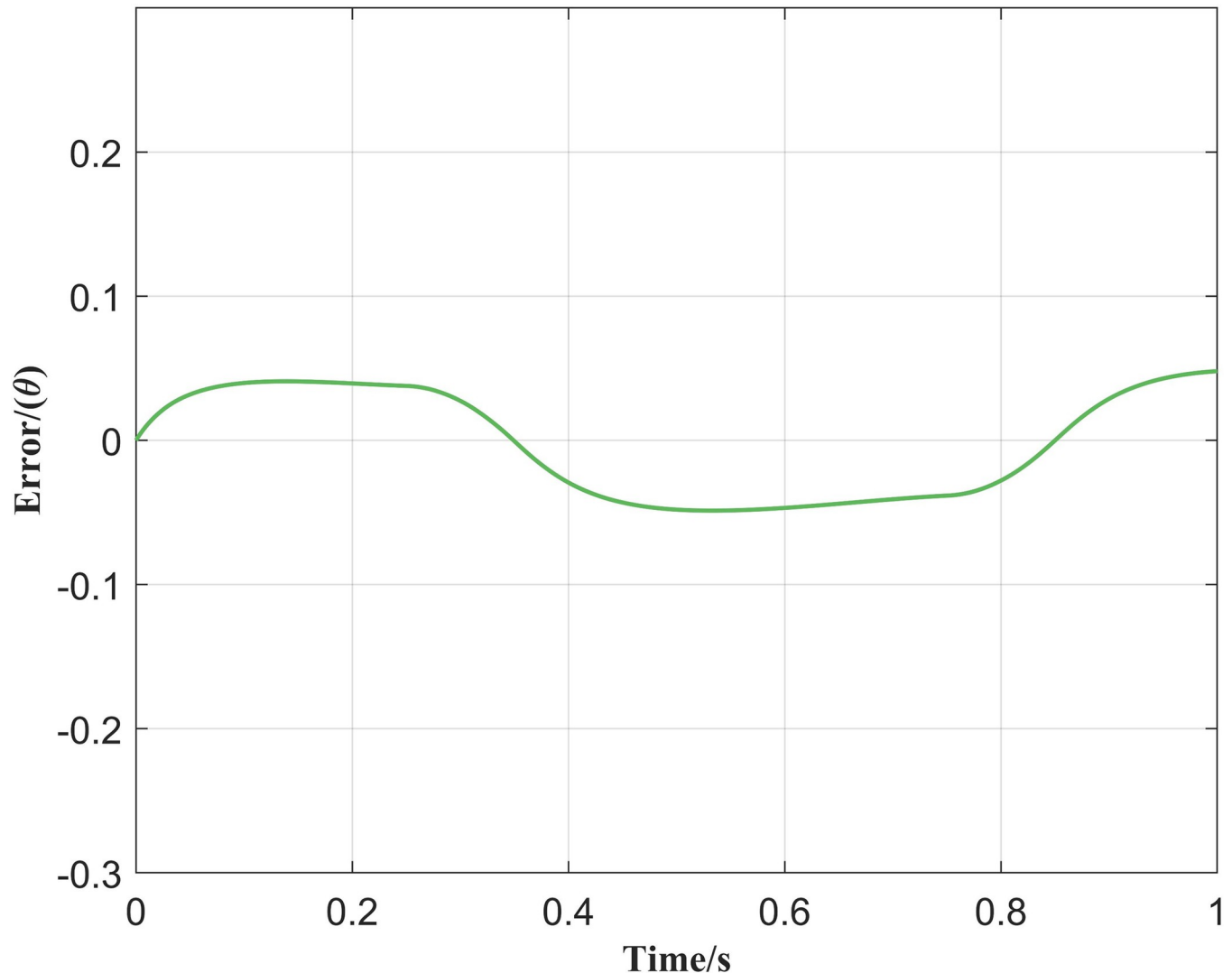
Fig 7. Corresponding position tracking error.

Fig 6 illustrates the position trajectory generated with the conventional PID controller and Fig 7 demonstrates the corresponding reference tracking error. It is clear that there is a bias between the reference trajectory and trajectory produced by the conventional PID controller. Therefore, the controller is unable to track the desired trajectories.

As can be seen from Fig 8, when the speed approaches zero, there is a static friction dominance whose change is multi-valued and discontinuous. This results in a noisy speed trajectory effected by the 'Stribeck' friction. The noise base fluctuations harm the PMSM and henceforth, they need to be compensated by the controller. However, the conventional PID controller is unable to handle such disturbances and therefore, this problem should be addressed by the adaptive control approaches.

We can compare the results of the P-ILC, PID and the proposed APD-ILC algorithms as in Fig 9. It is clear from the results that the conventional PID cannot accurately track the desired position. Even though the conventional P-ILC algorithm attempts to track the desired position, it eventually yields a noticeable tracking error. Thus, the error cannot be eliminated
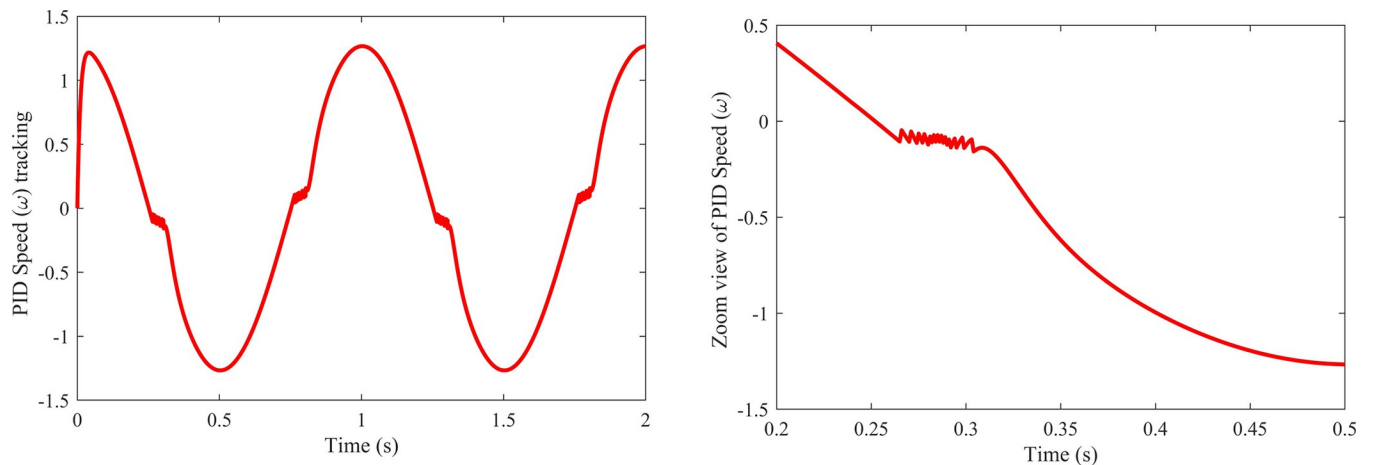
Fig 8. Speed trajectory with the conventional PID controller, left side shows whole speed trajectory, and right side shows partial speed trajectory with the Stribeck stemmed disturbance.

completely with the P-ILC as well. On the contrary, APD-ILC algorithm closely tracks the desired position and eliminates the friction effect to a large extent. Fig 10 shows the tracking errors where the error convergence with APD-ILC is superior since the it ultimately converges to zero, while the errors in other controllers (PID, P-ILC) remain non-zero.

Fig 11 shows the position tracking results with the APD-ILC for different iterations. It is clear that the tracking for 30th iteration y_{30} is more accurate than the 0th iteration y_0, 10th
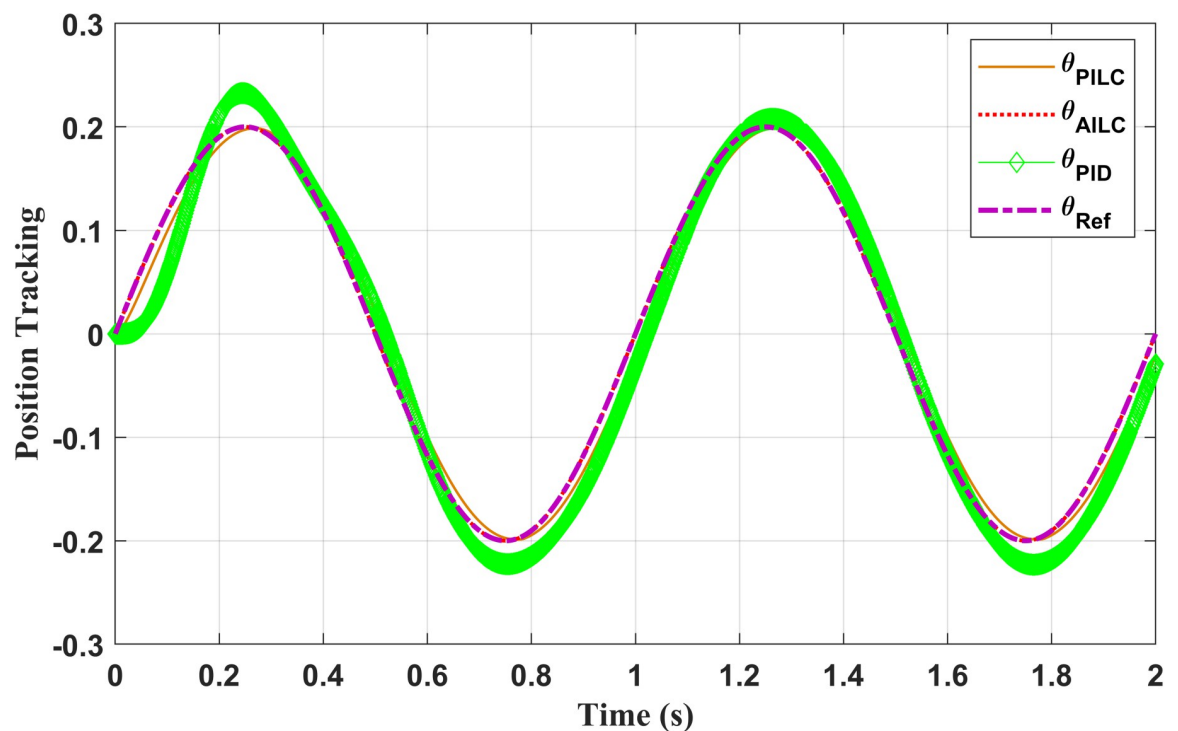
Fig 9. Performance comparison of the position tracking controllers.
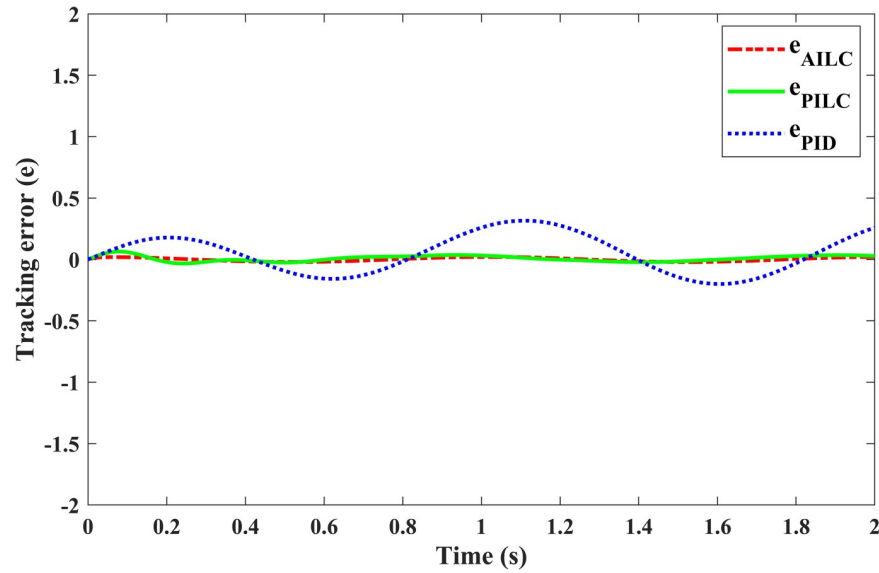
Fig 10. Corresponding error trajectories.

iteration y_{10} and 20th iteration y_{20}. Therefore, it can be stated that the tracking accuracy improves as the number of the iterations increase. It can be also noticed that the proposed APD-ILC offers proper friction compensation in the position tracking. The position tracking error curve is illustrated in Fig 12 also confirms the position tracking efficiency.

Fig 13 presents the speed tracking results for two different iterations; ω_0 is 0th iteration, ω_{20} is 20th iteration with respect to the reference speed ω_{ref}. It can be concluded from the figure
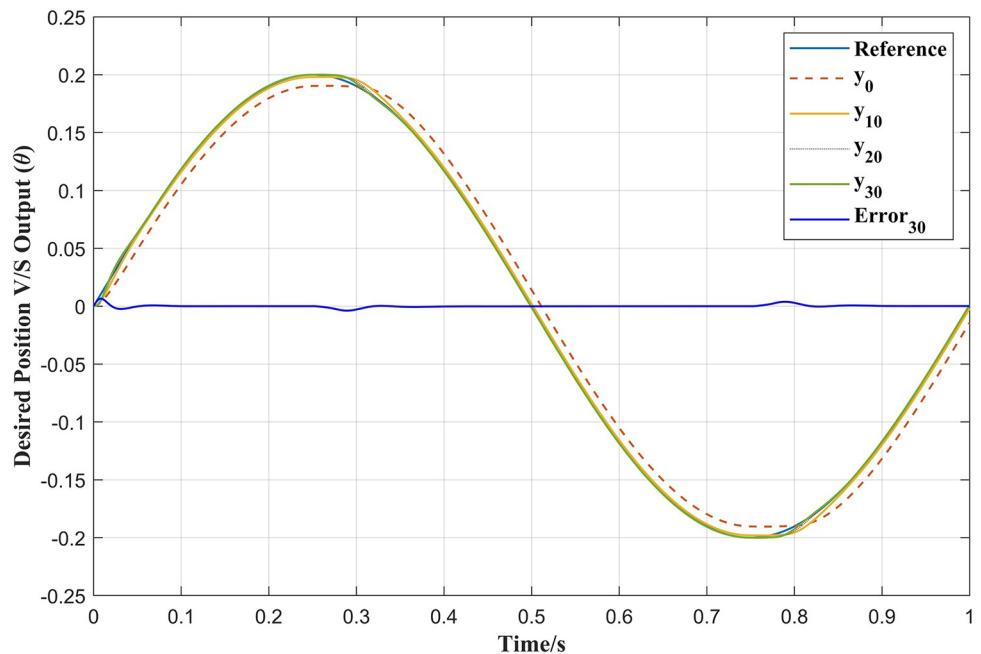
Fig 11. APD-ILC position tracking.
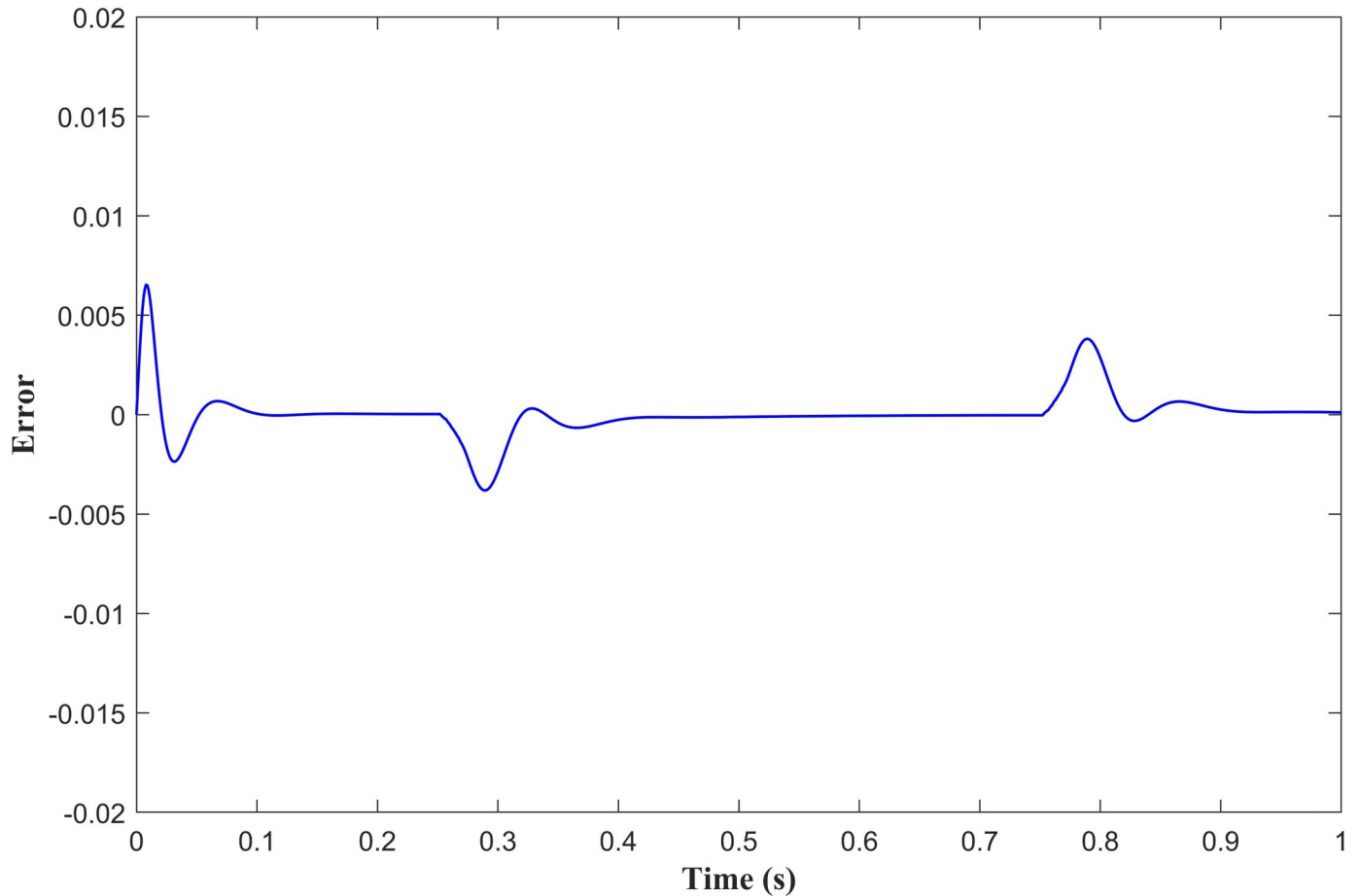
Fig 12. APD-ILC position tracking error.

that the friction compensation strategy dramatically improves the speed trajectory in the presence of the Stribeck friction.

Table 5 shows the position tracking errors for the P-ILC, PD-ILC and APD-ILC algorithms. It can be noticed that the proposed APD-ILC yields tracking error almost the half of the other control algorithms. After 20th iterations, the errors of P-ILC and PD-ILC algorithms produce 0.175381 and 0.024335 errors, respectively. It is clear that all the tracking errors reduce consecutively with the number of iterations increases. This occurs because all these control algorithms learn the unknown control parameters iteratively. The tracking error of the proposed APD-ILC algorithm is the smallest as compared to the other two control algorithms. Therefore, it can be easily observed from the Table 5 that the convergence speed of the proposed APD-ILC algorithm in this paper has significantly higher accuracy compared to other traditional control algorithms.

The position tracking error trajectories for the P-ILC, PD-ILC and APD-ILC algorithms are shown in Fig 14 with respect to the number of iterations. Due to the adaptive property of the APD-ILC algorithm, its RMS tracking error reduces quicker through the 30 iterations. Eventually, the tracking error converges to zero with increasing number of iterations which indicates that the proposed controller is efficient in dealing with motor nonlinearities and the Stribeck friction, particularly in servo control applications.
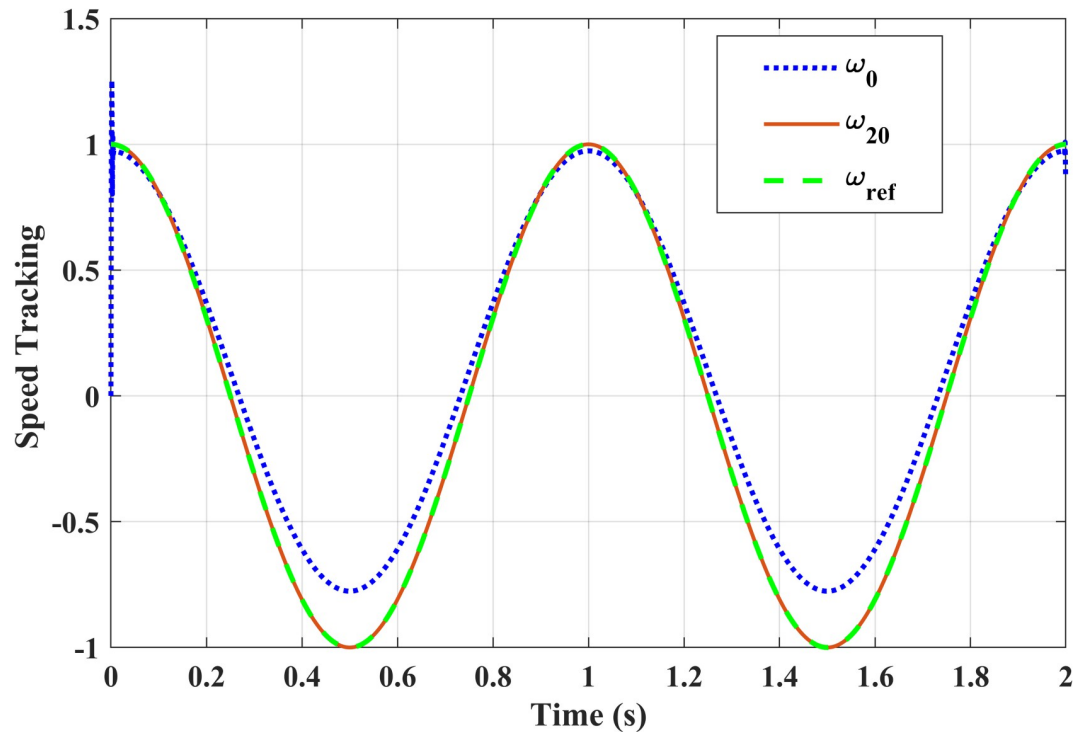
Fig 13. APD-ILC speed trajectories for different iterations.

https://doi.org/10.1371/journal.pone.0279253.g013

5. Conclusion

This paper proposed the APD-ILC algorithm to handle the Stribeck friction problem in the PMSM servo system. The genetic algorithm has been used to identify the nonlinear Stribeck friction unknown parameters with the offline training data and the constructed friction model was then used for the feedforward compensation. Finally, the APD-ILC algorithm has been designed to compensate the predicted Stribeck friction and also to track the desired position trajectory. An extensive comparison analyses has been performed to show the effectiveness and reliability of the proposed adaptive method. It was revealed that the conventional PID, P-ILC, PD-ILC algorithms were unable to overcome the friction disturbance properly, whereas the proposed APD-ILC was able consider the Stribeck friction and also eliminate it as desired. Thus, the proposed APD-ILC algorithm is robust and efficient to deal with the nonlinearities compared to the conventional control approaches. Other nonlinearities such as the parameter uncertainties in the servo system, gears backlash, and combined friction nonlinearity with external load disturbances can be considered in future research.

Table 5. Comparative values of tracking errors corresponding to ILC laws.

Iteration(k)	P-ILC	PD-ILC	APD-ILC
1st	7.21731636	7.11731545	3.28217325
5th	3.049819	2.598041	1.232084
10th	0.953581	0.584192	0. 29215
15th	0.375380	0.243351	0.003683
20th	0.175381	0.024335	0.001543

https://doi.org/10.1371/journal.pone.0279253.t006
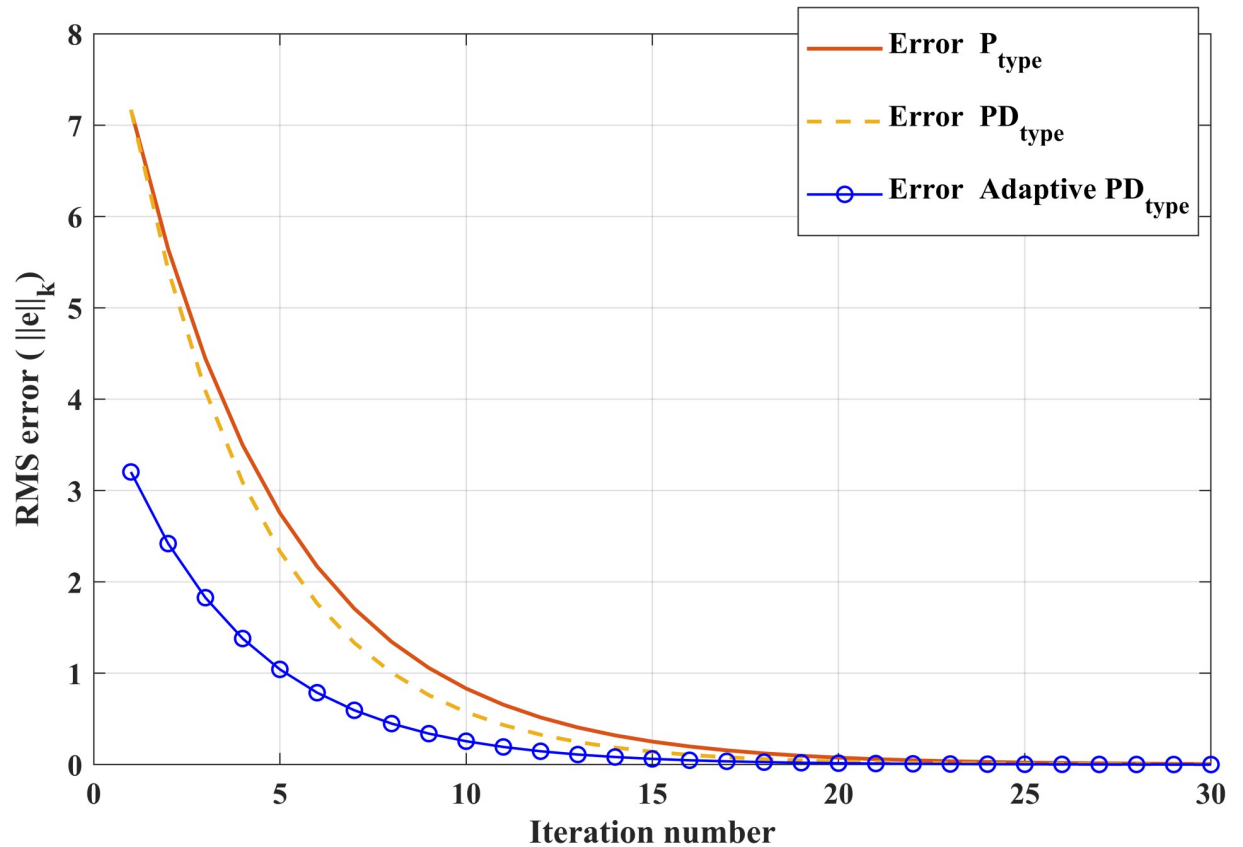
Fig 14. RMS error of the controllers for 30 iterations.

https://doi.org/10.1371/journal.pone.0279253.g014

Author Contributions

Conceptualization: Saleem Riaz.

Formal analysis: Saleem Riaz.

Investigation: Rong Qi.

Methodology: Saleem Riaz, Onder Tutsoy, Jamshed Iqbal.

Project administration: Rong Qi.

Resources: Jamshed Iqbal.

Supervision: Jamshed Iqbal.

Validation: Onder Tutsoy.

Visualization: Onder Tutsoy.

Writing – original draft: Saleem Riaz, Rong Qi.

Writing – review & editing: Onder Tutsoy, Jamshed Iqbal.

References

1. Ullah M.I., et al., Non-linear control law for articulated serial manipulators: Simulation augmented with hardware implementation. Elektronika ir Elektrotechnika, 2016. 22(1): p. 3–7. https://doi.org/10.5755/j01.eee.22.1.14094

2. Khan H., et al., Longitudinal and lateral slip control of autonomous wheeled mobile robot for trajectory tracking. Frontiers of Information Technology & Electronic Engineering, 2015. 16(2): p. 166–172.

3. Iqbal, J., S. Heikkila, and A. Halme. *Tether tracking and control of ROSA robotic rover*. in *2008 10th International Conference on Control, Automation, Robotics and Vision*. 2008. IEEE.

4. Iqbal J., et al., Towards sophisticated control of robotic manipulators: An experimental study on a pseudo-industrial arm. Strojniški vestnik-Journal of Mechanical Engineering, 2015. 61(7–8): p. 465–470. https://doi.org/10.5545/sv-jme.2015.2511

5. Alam W., et al., Nonlinear control of a flexible joint robotic manipulator with experimental validation. Strojniški vestnik-Journal of Mechanical Engineering, 2018. 64(1): p. 47–55. https://doi.org/10.5545/sv-jme.2017.4786

6. Jonnalagadda V.K. and Elumalai V.K., *Norm Optimal Iterative Learning Control for Improved Trajectory Tracking of Servo Motor*, in *Advances in Automation, Signal Processing, Instrumentation, and Control*. 2021, Springer. p. 1837–1845.

7. Riaz S., Lin H., and Akhter M.P., Design and implementation of an accelerated error convergence criterion for norm optimal iterative learning controller. Electronics, 2020. 9(11): p. 1766.

8. Tan C., Wang S., and Wang J., Robust iterative learning control for iteration-and time-varying disturbance rejection. International Journal of Systems Science, 2020. 51(3): p. 461–472.

9. Wang Z., et al., Online Iterative Learning Compensation Method Based on Model Prediction for Trajectory Tracking Control Systems. IEEE Transactions on Industrial Informatics, 2021.

10. Zhang C., Tian X., and Yan L., RBFNN-Based Nonuniform Trajectory Tracking Adaptive Iterative Learning Control for Uncertain Nonlinear System with Continuous Nonlinearly Input. Mathematical Problems in Engineering, 2021. 2021.

11. Sun, M., et al. *Adaptive Iterative Learning Control for Non-equal Length Tasks in the Presence of Initial Errors*. in *2021 IEEE 10th Data Driven Control and Learning Systems Conference (DDCLS)*. 2021. IEEE.

12. Riaz S., et al., An improved fast error convergence topology for PD α-type fractional-order ILC. Journal of Interdisciplinary Mathematics, 2021. 24(7): p. 2005–2019.

13. Cheng, Z. and Z. Zhuo. *Adaptive Iterative Learning Trajectory Tracking Control of SCARA Robot*. in *2021 IEEE 4th Advanced Information Management, Communicates, Electronic and Automation Control Conference (IMCEC)*. 2021. IEEE.

14. Wang J., et al., Continuous sliding mode iterative learning control for output constrained MIMO nonlinear systems q. Information Sciences, 2021. 556: p. 288–304.

15. Chen Q., et al., Adaptive repetitive learning control of PMSM servo systems with bounded nonparametric uncertainties: theory and experiments. IEEE Transactions on Industrial Electronics, 2020. 68(9): p. 8626–8635.

16. Wang L., Wu Z., and Liu C., Optimal parameter load disturbance compensation method of permanent magnet linear servo system. Diangong Jishu Xuebao(Transactions of China Electrotechnical Society), 2012. 27(3): p. 133–138.

17. Yang J., et al., Disturbance rejection for PMLSM based on iterative learning control and wavelet filter. Diangong Jishu Xuebao(Transactions of China Electrotechnical Society), 2013. 28(3): p. 87–92.

18. Liu C., et al., Research on thrust characteristics in permanent magnet linear synchronous motor based on analysis of nonlinear inductance. Proceedings of the CSEE, 2011. 30: p. 69–76.

19. Yan G., et al., PMLSM active disturbance rejection control. Diangong Jishu Xuebao(Transactions of China Electrotechnical Society), 2011. 26(9): p. 60–66.

20. DANG X., et al., Control for PMLSM based on wavelet neural network [J]. Electric Machines and Control, 2013. 17(1): p. 43–50.

21. Zheng W., et al., A Simplified Fractional Order PID Controller's Optimal Tuning: A Case Study on a PMSM Speed Servo. Entropy, 2021. 23(2): p. 130.

22. Zhong C.-Q., Wang L., and Xu C.-F., Path Tracking of Permanent Magnet Synchronous Motor Using Fractional Order Fuzzy PID Controller. Symmetry, 2021. 13(7): p. 1118.

23. Mechali, O., et al. *Finite-Time Attitude Control of Uncertain Quadrotor Aircraft via Continuous Terminal Sliding-Mode-Based Active Anti-Disturbance Approach*. in *2021 IEEE International Conference on Mechatronics and Automation (ICMA)*. 2021.

24. WANG L.-m., SHI J.-l., and XU C.-l., Robust control for permanent-magnet linear synchronous motor based on H_∞/LTR synthetic method [J]. Journal of Shenyang University of Technology, 2013. 3.

25. Zhang W., et al., An adaptive PID-type sliding mode learning compensation of torque ripple in PMSM position servo systems towards energy efficiency. ISA transactions, 2021. 110: p. 258–270.

26. Xia Z.-z. and Zhang G.-m., Design and evaluation of predictive functional control for a servo system. PROCEEDINGS-CHINESE SOCIETY OF ELECTRICAL ENGINEERING, 2005. 25(14): p. 130.

27. Zhang H., et al., Robust iterative learning control for permanent magnet linear motor. Electric Machines and Control, 2012. 16(6): p. 81–86.

28. Gong, Y., et al. *Iterative Learning Fault-Tolerant Control for Discrete-time Linear Switched Systems*. in *2021 IEEE 10th Data Driven Control and Learning Systems Conference (DDCLS)*. 2021. IEEE.

29. Teo C.-S., Tan K.-K., and Lim S.-Y., Dynamic geometric compensation for gantry stage using iterative learning control. IEEE Transactions on Instrumentation and measurement, 2008. 57(2): p. 413–419.

30. Zhu Y. and Zheng W.X., Multiple Lyapunov functions analysis approach for discrete-time-switched piecewise-affine systems under dwell-time constraints. IEEE Transactions on Automatic Control, 2019. 65(5): p. 2177–2184.

31. Zhu Y. and Zheng W.X., Observer-Based Control for Cyber-Physical Systems With Periodic DoS Attacks via a Cyclic Switching Strategy. IEEE Transactions on Automatic Control, 2020. 65(8): p. 3714–3721.

32. Selmic R.R. and Lewis F.L., Neural-network approximation of piecewise continuous functions: application to friction compensation. IEEE transactions on neural networks, 2002. 13(3): p. 745–751.

33. Guo X., et al. *Adaptive fuzzy control for permanent magnet spherical motor based on friction compensation*. in *Zhongguo Dianji Gongcheng Xuebao(Proceedings of the Chinese Society of Electrical Engineering)*. 2011. Chinese Society for Electrical Engineering.

34. Benxian, X., et al. *Study on nonlinear friction compensation for bi-axis servo system based-on ADRC*. in *International Conference on Information Science and Technology*. 2011. IEEE.

35. Ajwad S.A., et al., *Disturbance-observer-based robust control of a serial-link robotic manipulator using SMC and PBC techniques*. 2015. 24(4): p. 401–408.

36. Liu, S., J. Wang, and Z. Zheng. *Research on PMSM Speed Control System Based on Adaptive Fuzzy Control*. in *Journal of Physics: Conference Series*. 2021. IOP Publishing.

37. Ajwad S.A., et al., Disturbance-observer-based robust control of a serial-link robotic manipulator using SMC and PBC techniques. Studies in Informatics and Control, 2015. 24(4): p. 401–408.

38. Iwasaki M., Shibata T., and Matsui N., Disturbance-observer-based nonlinear friction compensation in table drive system. IEEE/ASME transactions on mechatronics, 1999. 4(1): p. 3–8.

39. Luo J., Wang L., and Liu B., Low-speed control of PMSM based on ADRC+ FOPID. Systems Science & Control Engineering, 2021. 9(1): p. 73–87.

40. Iqbal J., et al., Robotics inspired renewable energy developments: prospective opportunities and challenges. IEEE Access, 2019. 7: p. 174898–174923.

41. IQBAL J., KHAN Z.H., and KHALID A., Prospects of robotics in food industry. Food Science and Technology, 2017. 37(2): p. 159–165.

42. Jun Y., AN ANALOG COMPOUND ORTHOGONAL NEURAL NETWORK CONTROL OF THE SERVO SYSTEM IN FRICTION CONDITION [J]. Proceedings of the CSEE, 2005. 17.

43. Huang S. and Tan K.K., Intelligent friction modeling and compensation using neural network approximations. IEEE Transactions on Industrial Electronics, 2011. 59(8): p. 3342–3349.

44. Yue F. and Li X., Adaptive sliding mode control based on friction compensation for opto-electronic tracking system using neural network approximations. Nonlinear Dynamics, 2019. 96(4): p. 2601–2612.

45. Yue M., Wang L., and Ma T., Neural network based terminal sliding mode control for WMRs affected by an augmented ground friction with slippage effect. IEEE/CAA Journal of Automatica Sinica, 2017. 4(3): p. 498–506.

46. Tang X., et al., Neural membrane mutual coupling characterisation using entropy-based iterative learning identification. IEEE Access, 2020. 8: p. 205231–205243.

47. Zhang Q. and Sepulveda F., *Entropy-based axon-to-axon mutual interaction characterization via iterative learning identification*, in *EMBEC & NBC 2017*. 2017, Springer. p. 691–694.

48. Zhang, Q. and X. Dai. *Entropy-based iterative learning estimation for stochastic non-linear systems and its application to neural membrane potential interaction. in 2019 1st International Conference on Industrial Artificial Intelligence (IAI)*. 2019. IEEE.

49. Huang S., Liang W., and Tan K.K., Intelligent friction compensation: A review. IEEE/ASME Transactions on Mechatronics, 2019. 24(4): p. 1763–1774.

50. Park S. and Han S., Robust-tracking control for robot manipulator with deadzone and friction using backstepping and RFNN controller. IET control theory & applications, 2011. 5(12): p. 1397–1417.

51. Liu, C., et al. *A PMSM speed servo system based on internal model control with extended state observer. in IECON 2017-43rd Annual Conference of the IEEE Industrial Electronics Society*. 2017. IEEE.

52. Li S. and Gu H., Fuzzy adaptive internal model control schemes for PMSM speed-regulation system. IEEE Transactions on Industrial Informatics, 2012. 8(4): p. 767–779.

53. Ping Z., et al., Speed tracking control of permanent magnet synchronous motor by a novel two-step internal model control approach. International Journal of Control, Automation and Systems, 2018. 16 (6): p. 2754–2762.

54. Lu W., et al., A new load adaptive identification method based on an improved sliding mode observer for PMSM position servo system. IEEE Transactions on Power Electronics, 2020. 36(3): p. 3211–3223.

55. Gai, J.-t., et al. *A new fuzzy active-disturbance rejection controller applied in PMSM position servo system. in 2014 17th International Conference on Electrical Machines and Systems (ICEMS)*. 2014. IEEE.

56. Li L., et al., Robust position anti-interference control for PMSM servo system with uncertain disturbance. CES Transactions on Electrical Machines and Systems, 2020. 4(2): p. 151–160.

57. Sun X., et al., Design and implementation of a novel adaptive backstepping control scheme for a PMSM with unknown load torque. IET Electric Power Applications, 2019. 13(4): p. 445–455. https://doi.org/10.1049/iet-epa.2018.5656

58. Pennestrì E., et al., Review and comparison of dry friction force models. Nonlinear dynamics, 2016. 83 (4): p. 1785–1801.

59. Iqbal, J., N.G. Tsagarakis, and D.G. Caldwell. *A human hand compatible optimised exoskeleton system. in 2010 IEEE International Conference on Robotics and Biomimetics*. 2010. IEEE.

60. Dai M., et al., *PD-Type Iterative Learning Control with Adaptive Learning Gains for High-Performance Load Torque Tracking of Electric Dynamic Load Simulator*. 2021. 10(7): p. 811.